



Inhibiting Action of fruits of *Terminalia chebula* on 6063 aluminum alloy in sodium hydroxide solution

Deepa Prabhu, Padmalatha Rao^{1*}

¹Department of Chemistry, Manipal Institute of Technology, Manipal University, Karnataka 576104, India.

Received 14 June 2014, Revised 8 Jan 2015, Accepted 8 Jan 2015

*Corresponding Author. E-mail: drpadmalatharao@yahoo.com; Tel: (+91 9880122680)

Abstract

The inhibition characteristics of aqueous extract of fruits of *Terminalia chebula* (TCE) has been studied as a possible source of natural inhibitor for corrosion of 6063 aluminum alloy in sodium hydroxide solution by weight loss method and potentiodynamic polarization method. The effect of inhibitor was studied at different concentrations of medium (0.5 M, 1.0 M, 2.0 M), by varying inhibitor concentration and temperature in the range of 30 °C to 50 °C. Kinetic and Thermodynamic parameters were evaluated and discussed in detail. Inhibition efficiency increased with concentration of inhibitor and decreased with temperature as well as with the concentration of medium. The adsorption of TCE on metal surface obeyed the Langmuir adsorption isotherm. TCE acted as mixed inhibitor and followed physical adsorption on the surface of metal. The surface morphology of 6063 aluminum alloy, in absence and presence of TCE in 0.5 M sodium hydroxide were studied using scanning electron microscopy (SEM) and energy-dispersive X-ray spectroscopy (EDX).

Keywords: 6063 aluminum alloy, Potentiodynamic polarization, Weight loss, FT-IR spectroscopy, SEM-EDX

Introduction

Aluminum and its alloys represent an important material due to their wide range of industrial applications, especially in aerospace and household industries. The wide application of aluminum and aluminum alloys are due to their main properties like lightweight, formability, recyclability, corrosion resistance, durability, ductility and conductivity. These unique properties make them a valuable material. Aluminum is the most important metal second to iron in terms of production and consumption [1,2]. The good corrosion resistance of aluminum and its alloys is attributable to a thin oxide film that forms on aluminum upon exposure to the atmosphere or aqueous solutions that protects the metal from further oxidation. When it is exposed to acid or alkaline condition that destroys this protective coating there by corrosion of aluminum occurs [3].

Sodium hydroxide solution is used for cleaning and degreasing process [2, 4]. One of the important methods against the corrosion is to use inhibitors. The effect of inhibitor is to reduce the corrosion of metal or to modify the electrode reactions that cause dissolution of metal. Most of the efficient acid inhibitors are organic compounds that contain mainly nitrogen, sulfur or oxygen atoms in their structure. The inhibition efficiency of these compounds is dependent on the structure and chemical properties of the layer formed on the surface of metal.

Literature is available for the corrosion inhibition of aluminum in NaOH using organic inhibitor [5-8]. Recently, the use of chemical inhibitors has been limited due to environmental regulations. Among numerous inhibitors, eco-friendly corrosion inhibitors are preferred. Plant extracts have gained importance because they are eco-friendly and renewable source. The plant extracts are the source of chemical compounds that can be extracted by simple procedures with low cost.

Some plant extracts have been used as effective corrosion inhibitors of steel and aluminum in acidic and alkaline media [9-11]. Abdel-Gaber et al. [12] proposed the effect of natural extract for the corrosion inhibitor for aluminum in NaOH solutions. The available literature for the use of plant extract as a corrosion inhibitor for 6063 aluminum alloy in NaOH solution is less studied [13,14]. Therefore, it is required to extend the study of plant extract as corrosion inhibitors for 6063 aluminum alloy in sodium hydroxide solutions. In the present

work, *Terminalia chebula* extract is chosen to be the corrosion inhibitor for corrosion control of 6063 aluminum alloy in sodium hydroxide solution. *Terminalia chebula* is a tree belonging to Combretaceae family. Fruit of *Terminalia chebula* are used widely in medicine. *Terminalia chebula* fruits contain several biodegradable ecologically acceptable organic compounds [15]. No reported literature is available for using *Terminalia chebula* for the corrosion control of 6063 aluminum alloy in sodium hydroxide solution.

2. Materials and methods

2.1. Material and preparation of test coupons

The experiments were performed with specimen of 6063 aluminum alloy. The composition of the material is 0.59% of Si, 0.31% of Mg, 0.12% of Fe and 98.9% of Al. Cylindrical test coupons were sealed with Acrylic resin material in such a way that the area exposed to the medium was 1.0 cm² of 6063 aluminum alloy. It was polished with 180, 280, 400, 600, 800, 1000, 1500, and 2000 grade emery papers. Further polishing was done with disc polisher using levigated alumina to get mirror surface. It was then dried and stored in a desiccator to avoid moisture before corrosion studies.

2.2. Preparation of medium

Analytical grades (Merck) of sodium hydroxide solution and doubly distilled water were used for preparing the test solutions (0.5 M, 1.0 M, 2.0 M). Stock solution of higher concentration was prepared, standardized and used. All experiments were carried out under thermostatic conditions between 30 °C, 35 °C, 40 °C, 45 °C, 50 °C (±0.5 °C).

2.3. Preparation of inhibitors

A sample of the powder (25 g) was refluxed in 250 ml of water at 90 °C for 3 h. The refluxed solution was kept overnight [16], filtered and the filter liquor was evaporated to dryness. Then the deep brown-reddish solid residue was obtained, and preserved in a desiccator. It was used to prepare the inhibitor solution of required strength in distilled water. The concentration range of TCE used was in Parts per million (ppm).

2.4. Fourier transform infrared (FT-IR) spectroscopy

The dried powder of TCE was characterized by FT-IR spectroscopy. The spectrum of the dried sample was recorded using spectrophotometer (Shimadzu Model) in the frequency range of 4000 to 400 cm⁻¹ using KBr pellet technique.

2.5. Corrosion inhibition studies of 6063 aluminum alloy in sodium hydroxide solution

2.5.1. Weight loss method

The procedure for weight loss determination was similar to that reported earlier [18]. The coupons were weighed and their initial weight recorded before immersion in 250 mL open beakers containing 100 mL of 0.5 M, 1.0 M and 2.0 M NaOH as corroding and the addition of different concentrations of the inhibitor extract at 30°C. The variation of weight loss was monitored after 2 h immersion per coupon. After 2 h, the coupons were taken out, immersed in concentrated nitric acid at room temperature, scrubbed with a bristle brush under running water, dried and reweighed. Triplicate experiments were performed in each case. Each reading reported is an average of three experimental readings recorded to the nearest 0.0001 g on a digital analytical balance. Percentage inhibition efficiency IE (%) was calculated using the following equation (1).

$$IE(\%) = \frac{W_0 - W_1}{W_0} \times 100 \quad (1)$$

where W_0 and W_1 are the weight loss obtained in uninhibited and inhibited solutions, respectively.

2.5.2. Potentiodynamic polarization studies

Electrochemical measurements were carried out by using an electrochemical work station (CH600D-series, U.S. Model with CH instrument beta software). Both polarization studies were carried using conventional three-electrode Pyrex glass cell with a platinum counter electrode and saturated calomel electrode (SCE) as reference electrode. The working electrode was made up of 6063 aluminum alloy. All the values of potential were measured with reference to the saturated calomel electrode.

Finely polished specimen of 6063 aluminum alloy were exposed to corrosive medium at different temperature in the range of 30 °C to 50 °C. The potentiodynamic current-potential curves were recorded by polarizing the specimen to -250 mV cathodically and +250 mV anodically with respect to open circuit potential (OCP) at a scan rate of 0.01 V/s.

Inhibitor efficiency was calculated using the equation (2):

$$IE(\%) = \frac{i_{\text{corr}} - i_{\text{corr(inh)}}}{i_{\text{corr}}} \times 100 \quad (2)$$

where i_{corr} and $i_{\text{corr(inh)}}$ are the corrosion current densities obtained in uninhibited and inhibited solutions, respectively. The corrosion rate was calculated using equation (3) [17]:

$$CR(\text{mm y}^{-1}) = \frac{3.27 \times M \times i_{\text{corr}}}{\rho \times Z} \quad (3)$$

where 3.27 is a constant that defines the unit of corrosion rate, i_{corr} is the corrosion current density in A cm^{-2} , ρ is the density of the corroding material (g cm^{-3}), M is the atomic mass of the metal and Z is the number of electrons transferred per atom.

2.6. Calculations of kinetic, thermodynamic and adsorption isotherm studies

The value of activation energy (E_a) were calculated [19] using the Arrhenius equation (4)

$$\ln(CR) = B - \frac{E_a}{RT} \quad (4)$$

where B is a constant which depends on the metal type, R is the universal gas constant, and T is the absolute temperature.

$$CR = \frac{RT}{Nh} \exp\left(\frac{\Delta S^\ddagger}{R}\right) \exp\left(\frac{\Delta H^\ddagger}{RT}\right) \quad (5)$$

where h is Plank's constant and N is Avagadro's number. The enthalpy and entropy of activation for the dissolution of the alloy, (ΔH^\ddagger & ΔS^\ddagger) were calculated from transition state theory equation (5).

The adsorption of an organic adsorbate at metal/solution interface can be presented as a substitution adsorption process between the organic molecules in aqueous solution (Inh_{aq}), and the water molecules on metallic surface ($\text{H}_2\text{O}_{\text{ads}}$), as given in equation (6):



where χ , the size ratio, is the number of water molecules displaced by one molecule of organic inhibitor. χ is assumed to be independent of coverage or charge on the electrode. In order to obtain an isotherm, the linear relation between the surface coverage (θ) value and concentration of the inhibitor (C_{inh}) must be found. The surface coverage θ is given by equation (7).

$$\theta = \frac{\text{IE}(\%)}{100} \quad (7)$$

Where $\text{IE}(\%)$ is the percentage inhibition efficiency.

The values of θ at different concentrations of inhibitor in the solution (C_{inh}) were applied to various isotherms including Langmuir, Temkin, Frumkin and Freundlich isotherms. It was found that the experimental data fitted best with the Langmuir adsorption isotherm.

Langmuir adsorption isotherm, which is given by the equation (8):

$$\frac{C_{\text{inh}}}{\theta} = C_{\text{inh}} + \frac{1}{K} \quad (8)$$

where K is the adsorption/desorption equilibrium constant, C_{inh} is the corrosion inhibitor concentration in the solution, and θ is the surface coverage. The plot of C_{inh}/θ versus C_{inh} gives a straight line with an intercept of $1/K$.

2.7. Scanning electron microscopy (SEM) and Energy-dispersive X-ray spectroscopy (EDX) analysis

The scanning electron microscope images were recorded to establish the interaction of sodium hydroxide solution as well as inhibitor with the metal surface using EVO 18-15-57 scanning electron microscope with Energy-dispersive X-ray spectroscopy. The surface morphology of 6063 aluminum alloy immersed in the presence of inhibitor (TCE) was compared with that of corroded sample of the 6063 aluminum alloy in sodium hydroxide (0.5 M) solution. The EDX images give the information of the percentage composition of elements present over the surface of the metal, before and after inhibition in the corrosive medium.

3. Results and discussion

3.1. Fourier transform infrared (FT-IR) spectroscopy

Fig.1 shows the FTIR spectrum of TCE. $-\text{OH}$ stretching frequency appears at 3417 cm^{-1} . The aromatic stretching frequency appears at 2923 cm^{-1} and 2852 cm^{-1} . COO stretching frequency is at 2368 cm^{-1} . $-\text{C}=\text{O}-$ stretching frequency is at 1720 cm^{-1} . $-\text{C}=\text{C}-$ stretching frequency at 1620 cm^{-1} . $-\text{CH}_2$ bending frequency 1458 cm^{-1} and 1350 cm^{-1} . $-\text{C}-\text{O}$ bending frequency at 1211 cm^{-1} . $-\text{C}=\text{C}-$ bending frequency at 1026 cm^{-1}

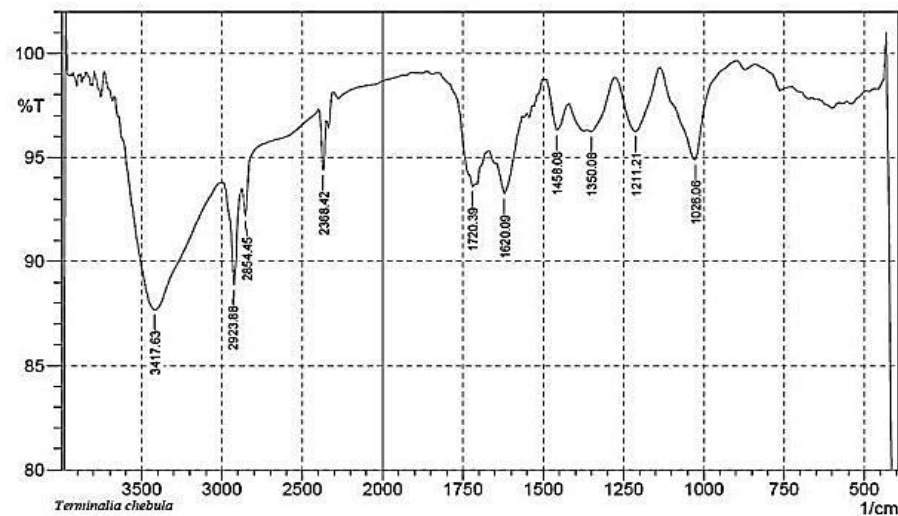


Figure 1: FTIR spectra of solid residue of TCE

3.2. Corrosion inhibition studies of TCE on 6063 aluminum alloy in Sodium hydroxide solution

3.2.1. Weight loss method

The weight loss study was performed with various concentrations of TCE, to study the influence of various concentrations of TCE on the corrosion inhibition of 6063 aluminum alloy in NaOH solution at 30°C for a period of two hours. The corrosion parameters obtained from weight loss measurements for 6063 aluminum alloy in NaOH solution containing various concentrations of TCE are listed as Table 1. It was found that with the rise in concentration of TCE, the weight loss of 6063 aluminum alloy decreased, and the inhibition efficiency increased. Beyond the optimum concentration of inhibitor, there is no improvement in the inhibition efficiency. The variation of inhibition efficiency with various concentrations of TCE on 6063 aluminum alloy in NaOH is shown as Fig. 2.

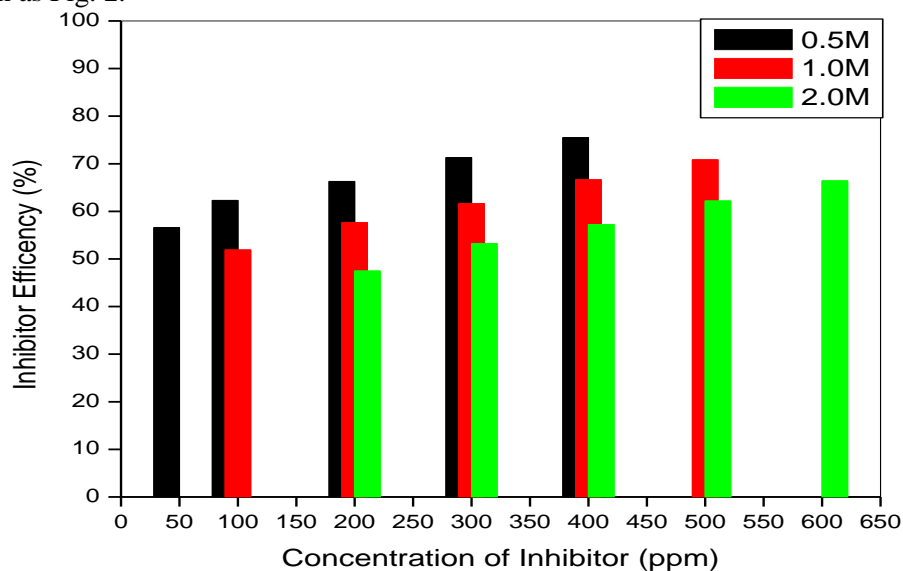


Figure 2: The variation of inhibition efficiency with various concentrations of TCE on 6063 aluminum alloy in NaOH

3.2.2. Potentiodynamic polarization measurements

The potentiodynamic polarization plots for the corrosion of 6063 aluminum alloy specimen in 0.5 M NaOH in the presence of different concentrations of TCE, at 30 °C are shown in the Fig. 3. Similar plots were obtained at different temperatures studied. The potentiodynamic polarization parameters obtained from these plots in 6063 aluminum alloy in sodium hydroxide in the presence of different concentrations of TCE at different temperatures and different strengths of NaOH are given in Tables 2 to Table 4.

Table 1: Results of weight loss measurements of 6063 aluminium alloy in NaOH solution containing various concentrations of TCE

NaOH (M)	Conc. of inhibitor (ppm)	Weight loss (mg)	CR (mm y ⁻¹)	I.E (%)
0.5	Blank	129.8	32.23	
	50	56.36	14.00	56.58
	100	48.92	12.15	62.31
	200	43.73	10.86	66.31
	300	37.24	9.25	71.31
	400	31.79	7.89	75.51
1.0	Blank	260.2	74.30	
	100	125.13	31.07	51.91
	200	110.22	27.37	57.64
	300	99.81	24.79	61.64
	400	86.80	21.56	66.64
	500	75.87	18.84	70.84
2.0	Blank	370.74	92.06	
	200	194.68	48.34	47.49
	300	173.43	43.07	53.22
	400	158.49	39.36	57.25
	500	140.18	34.81	62.19
	600	124.49	30.92	66.42

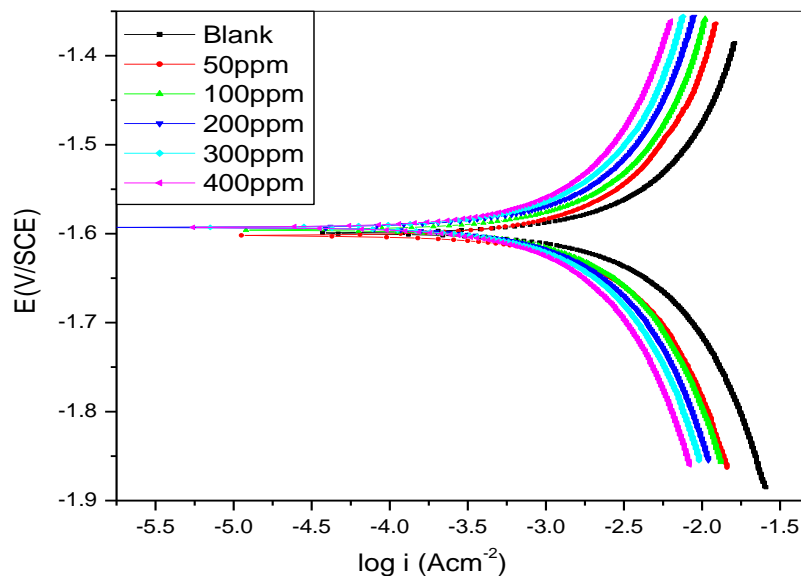


Figure 3: Tafel polarization curves for the corrosion of 6063 aluminium alloy in 0.5 M sodium hydroxide containing different concentrations of TCE at 30 °C.

The i_{corr} decreased significantly even on the addition of a small concentration of TCE. Inhibition efficiency (IE%) increases with the increase in the inhibitor concentration, up to an optimum value. It is seen from Table 2 to Table 4 that the value of b_c does not change significantly with the increase in TCE concentration, which indicates that the addition of TCE does not change the hydrogen evolution reaction mechanism [18]. It is also seen from the data that the anodic slope b_a also does not change significantly on increasing the concentration of TCE, indicating its non-interference in the mechanism of anodic reaction. The barrier film formed on the metal surface reduces the probability of both the anodic and cathodic reactions, which results in decrease in corrosion rate [19,20]. There is no appreciable shift in the corrosion potential value (E_{corr}) on the addition of TCE to the corrosion medium and also on increasing the concentration of TCE. The maximum displacement in the present study is less than ± 85 mV, which indicates that TCE is a mixed type inhibitor [19,21].

It is seen that the inhibition efficiency decreased with temperature increase. These results reveal the physisorption of the inhibitor molecules on the 6063 aluminum alloy surface in sodium hydroxide also.

Table 2: Electrochemical parameters obtained from potentiodynamic polarization measurements of 6063 Al alloy in 0.5 M sodium hydroxide at various concentrations of TCE

Temp (°C)	Conc. of inhibitor (ppm)	E_{corr} (mV vs SCE)	i_{corr} (m A cm ⁻²)	β_a (m V dec ⁻¹)	$-\beta_c$ (m V dec ⁻¹)	CR (mm y ⁻¹)	η (%)
30	Blank	-1594	3.26	485	472	35.53	-
	50	-1593	1.32	484	492	14.36	59.60
	100	-1590	1.13	486	477	12.32	65.33
	200	-1593	1.00	485	469	10.90	69.33
	300	-1586	0.84	496	459	9.12	74.33
	400	-1593	0.70	492	455	7.63	78.53
35	Blank	-1610	3.74	479	503	40.77	-
	50	-1596	1.68	472	486	18.35	54.99
	100	-1595	1.47	474	485	16.01	60.72
	200	-1597	1.30	478	484	14.18	65.22
	300	-1596	1.09	483	483	11.92	70.75
	400	-1593	0.94	485	480	10.26	74.84
40	Blank	-1611	4.24	489	489	46.22	-
	50	-1602	2.09	482	476	22.81	50.64
	100	-1600	1.79	483	474	19.52	57.77
	200	-1601	1.64	485	471	17.83	61.43
	300	-1598	1.41	487	470	15.41	66.65
	400	-1596	1.24	490	469	13.52	70.74
45	Blank	-1622	4.55	480	478	49.60	-
	50	-1607	2.44	479	467	26.64	46.29
	100	-1605	2.20	480	465	24.03	51.55
	200	-1604	2.05	478	464	22.38	54.87
	300	-1602	1.82	476	461	19.84	60
	400	-1604	1.54	475	460	16.81	66.11
50	Blank	-1623	5.50	488	480	59.95	-
	50	-1613	3.19	486	469	34.78	41.99
	100	-1610	2.89	489	467	31.51	47.44
	200	-1609	2.65	490	464	28.90	51.80
	300	-1606	2.41	493	463	26.25	56.22
	400	-1610	2.13	496	431	23.18	61.33

3.3. Effect of temperature

The study of the effect of temperature on the corrosion rate and inhibition efficiency facilitates the calculation of kinetic and thermodynamic parameters for corrosion and inhibition processes.. In the current investigation the results indicated that inhibition efficiency of TCE decreased with the increase in temperature. The increase in solution temperature, did not alter the corrosion potential (E_{corr}), anodic Tafel slope (β_a) and cathodic Tafel slope (β_c) values significantly. This is clear indication of the fact that the increase in temperature may not alter the mechanism of corrosion reaction [22]. However, i_{corr} and hence the corrosion rate of the specimen increased with the increase in temperature for both blank and inhibited solutions. The decrease in inhibition efficiency with the increase in temperature may be attributed to the higher dissolution rates of 6063 aluminum alloy at

elevated temperature. The decrease in inhibition efficiency with the increase in temperature is also suggestive of physical adsorption of the inhibitor molecules on the metal surface [23]. The Arrhenius plots for the corrosion of 6063 aluminum alloy in presence of different concentrations of TCE in 0.5 M sodium hydroxide solution are shown in Fig. 4

Table 3: Electrochemical parameters obtained from potentiodynamic polarization measurements of 6063 Al alloy in 1.0 M sodium hydroxide at various concentrations of TCE

Temp (°C)	Conc. of inhibitor (ppm)	E_{corr} (mV vs SCE)	i_{corr} (m A cm ⁻²)	β_a (m V dec ⁻¹)	$-\beta_c$ (mV dec ⁻¹)	CR (mm y ⁻¹)	η (%)
30	Blank	-1645	6.93	466	515	75.54	-
	100	-1607	3.09	448	494	33.66	55.44
	200	-1605	2.69	445	509	29.33	61.17
	300	-1605	2.41	454	500	26.31	65.17
	400	-1601	2.07	425	517	22.53	70.17
	500	-1597	1.78	422	496	19.36	74.37
35	Blank	-1634	7.94	457	504	86.55	-
	100	-1609	3.90	505	489	42.55	50.83
	200	-1609	3.45	442	485	37.60	56.56
	300	-1605	3.09	461	483	33.70	61.06
	400	-1600	2.65	430	502	28.92	66.59
	500	-1603	2.33	452	508	25.38	70.68
40	Blank	-1633	8.57	471	511	93.41	-
	100	-1614	4.59	481	492	49.99	46.48
	200	-1613	3.98	447	475	43.33	53.61
	300	-1609	3.66	464	502	39.92	57.27
	400	-1609	3.21	453	499	35.04	62.49
	500	-1607	2.86	441	496	31.22	66.58
45	Blank	-1646	9.20	486	510	100.28	-
	100	-1618	5.32	475	499	58.03	42.13
	200	-1610	4.84	467	497	52.76	47.39
	300	-1604	4.53	475	495	49.43	50.71
	400	-1605	4.06	481	506	44.28	55.84
	500	-1606	3.50	443	404	38.16	61.95
50	Blank	-1647	11.25	491	443	122.63	-
	100	-1619	6.99	460	510	76.24	37.83
	200	-1618	6.38	487	493	69.55	43.28
	300	-1617	5.89	487	482	64.21	47.64
	400	-1614	5.39	465	461	58.79	52.06
	500	-1615	4.82	450	487	52.52	57.17

Table 4: Electrochemical parameters obtained from potentiodynamic polarization measurements of 6063 Al alloy in 2.0 M sodium hydroxide at various concentrations of TCE

Temp (°C)	Conc. of inhibitor (ppm)	E_{corr} (mV vs SCE)	i_{corr} (mA cm ⁻²)	β_a (mV dec ⁻¹)	$-\beta_c$ (mV dec ⁻¹)	CR (mm y ⁻¹)	η (%)
30	Blank	-1656	8.55	577	533	93.2	-
	200	-1618	4.21	471	518	45.94	50.71
	300	-1612	3.72	457	528	40.60	56.44
	400	-1601	3.38	452	527	36.87	60.44
	500	-1606	2.95	444	534	32.21	65.44
	600	-1608	2.60	471	536	28.29	69.64
35	Blank	-1661	9.51	533	524	103.66	-
	200	-1621	5.13	463	496	55.87	46.1
	300	-1620	4.58	448	526	49.93	51.83
	400	-1596	4.15	461	498	45.27	56.33
	500	-1614	3.63	463	469	39.54	61.86
	600	-1618	3.24	463	496	35.30	65.95
40	Blank	-1661	10.18	545	527	110.96	-
	200	-1622	5.93	493	512	64.64	41.75
	300	-1624	5.20	466	513	56.72	48.88
	400	-1619	4.83	542	514	52.66	52.54
	500	-1612	4.30	475	515	46.87	57.76
	600	-1628	3.88	493	512	42.33	61.85
45	Blank	-1664	11.78	555	498	128.4	-
	200	-1611	7.37	494	515	80.38	37.4
	300	-1619	6.75	495	508	73.63	42.66
	400	-1614	6.36	477	524	69.36	45.98
	500	-1598	5.76	484	531	62.78	51.11
	600	-1621	5.04	494	530	54.93	57.22
50	Blank	-1666	12.55	538	480	136.8	-
	200	-1622	8.40	499	512	91.52	33.1
	300	-1621	7.71	501	484	84.06	38.55
	400	-1628	7.16	482	538	78.10	42.91
	500	-1610	6.61	513	497	72.05	47.33
	600	-1596	5.97	512	513	65.06	52.44

Plots of $\ln(\text{CR}/T)$ versus $1/T$ for the corrosion of 6063 aluminum alloy in the presence of different concentrations of TCE in 0.5 M sodium hydroxide solution are shown in Fig. 5. The calculated values of activation parameters are given Table 5. The increase in apparent activation energy may be interpreted as due to physical adsorption [23, 24] of the inhibitor and is in agreement with enthalpy of activation. Large negative values of entropies show that the activated complex in the rate determining step is an association rather than dissociation step meaning that a decrease in disordering takes place on going from reactants to the activated complex [25].

The adsorption of the inhibitor on the electrode surface leads to the formation of a barrier between the metal surface and the corrosion medium, and thereby reducing the metal reactivity [26].

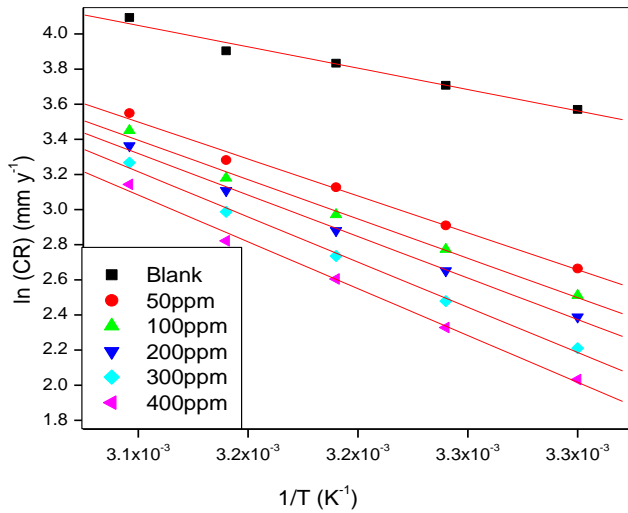


Figure 4: Arrhenius plots for the corrosion of 6063 aluminum alloy in 0.5 M sodium hydroxide containing different concentrations of TCE

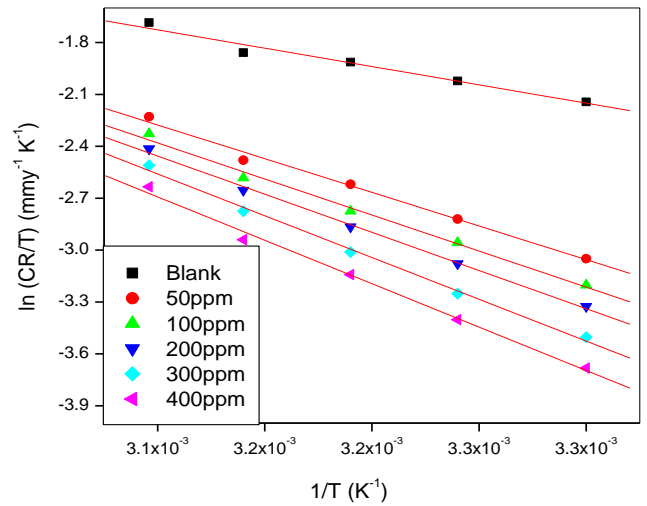


Figure 5: Plots of $\ln(CR/T)$ vs $1/T$ for the corrosion of 6063 aluminum alloy in 0.5 M sodium hydroxide containing different concentrations of TCE

3.4. Adsorption behavior

The information on the interaction between the inhibitor molecules and the metal surface can be provided by adsorption isotherm [27]. Fig.6 represents the Langmuir adsorption isotherms for the adsorption of TCE on the 6063 aluminum alloy surface in 0.5 M NaOH. The plots were linear, with an average correlation coefficient (R^2) of 0.99. The Langmuir isotherm equation is based on the assumption that adsorbed molecules do not interact with one another. In aqueous extract of TCE, numerous organic heterocyclic compounds are present along with the principal active components and they may also get adsorbed over the metal surface. Such adsorbed species may interact by mutual repulsion or attraction. Hence the slope values of the adsorption isotherms deviate from unity. Therefore it is safely recommended to not determine standard free energy of adsorption (ΔG^0_{ads}) values and other thermodynamic parameters [28].

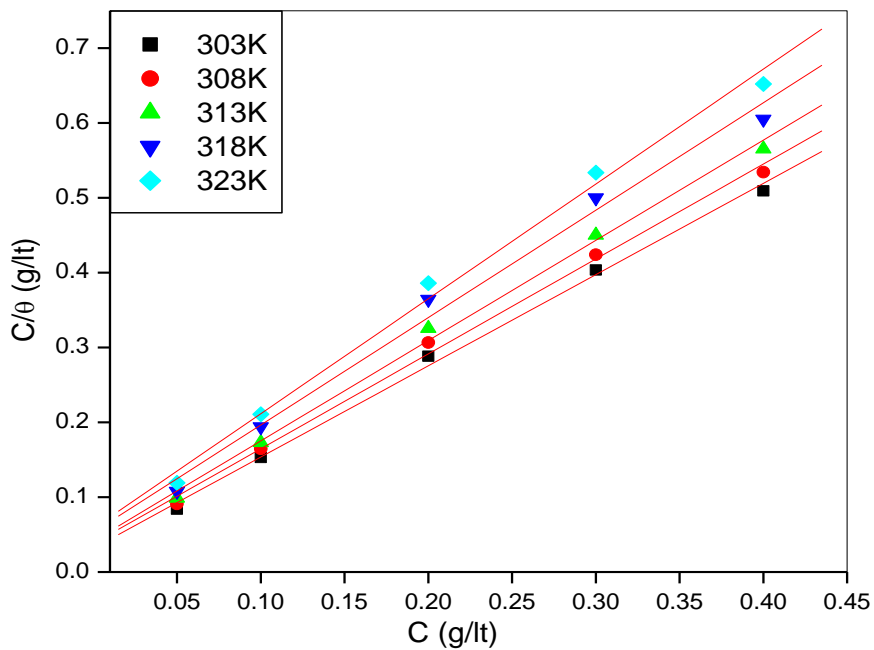


Figure 6: Langmuir adsorption isotherms for the adsorption of TCE on 6063 aluminium alloy in 0.5 M sodium hydroxide at different temperatures

3.5. Explanation for inhibition

Nature and structure of inhibiting molecules play a vital role in controlling the corrosion of the metal surface. The adsorption mechanism for a given inhibitor depends on factors, such as the nature of the metal, the corrosive medium, the pH, and the concentration of the inhibitor as well as the functional groups present in its molecule, since different groups are adsorbed to different extents [29].

TCE consists of a number of glycosides, triterpenes (arjunglucoside I, arjungenin, and the chebulosides I and II). Principal active constituents are reported to be chebulin, and phenolic compounds including chebulinic acid [30, 31]. The structures of principal constituents of TCE are shown in Fig. 9.

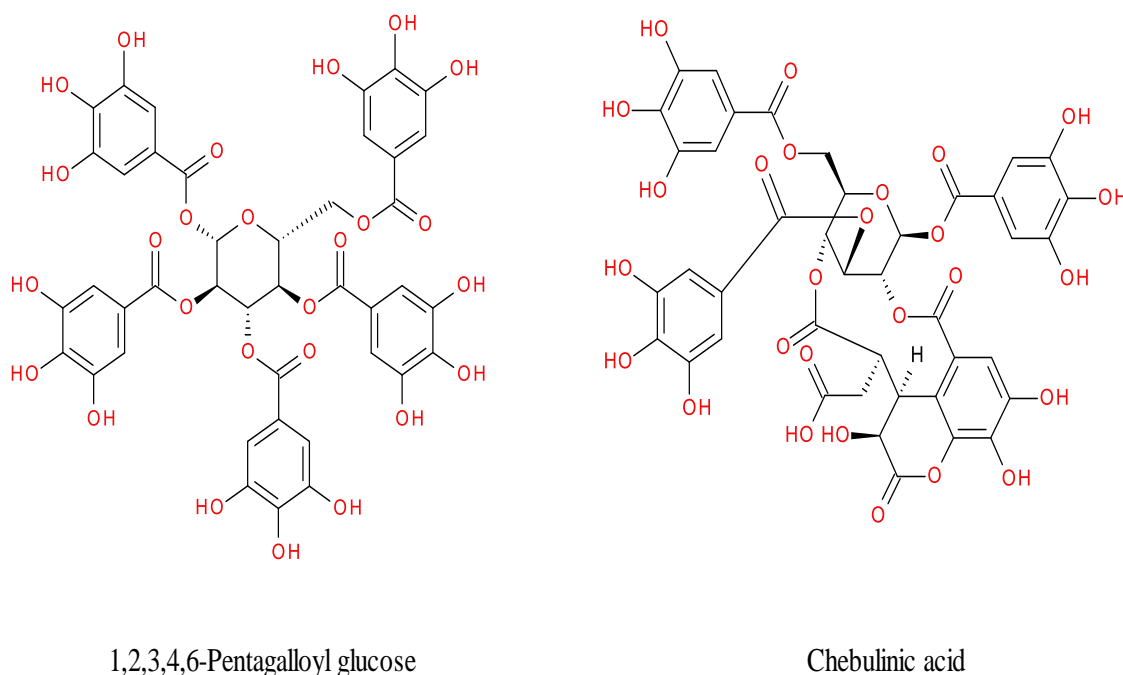
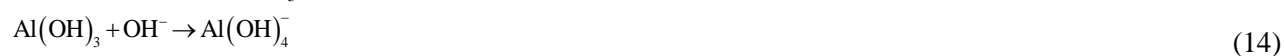


Figure 9: Constituents of TCE

The inhibitive effect of TCE on the corrosion of aluminum can be accounted for on the basis of its adsorption on the surface. The adsorption of TCE molecules on the metal surface can be attributed to the presence of electronegative elements like oxygen and also to the presence of π -electron cloud in the benzene ring of the molecule. Increase in inhibition efficiencies with increase in inhibitor concentration shows that the inhibition action is due to the adsorption on the aluminum surface. Adsorption may take place by organic molecules at metal/solution interface due to bonding between the charged molecules and charged metal, interaction of unshared electron pairs in the molecule with the metal, interaction of π - electrons with the metal or the combination of the above [31- 38].

The corrosion involves the electrochemical process resulting from dissolution of Al metal [3, 4] in the alkali. This process can be expressed by anodic and cathodic processes.

Anodic process:



Cathodic process: It is the reduction of water molecule.



On the other hand, hydrogen evolution takes place simultaneously with the dissolution of aluminum metal. The observation of gas bubbles on the corroding aluminum surface shows that the corrosion of aluminum in alkaline solution proceeds mainly by water reduction [3].

The presence of magnesium, silicon along with amount of iron to aluminum produces the compound magnesium-silicide (Mg_2Si) and $AlFeSi$. In addition to these there will be silicon (Si) in aluminum matrix. Electrochemical behavior of the various phase are different from that of matrix. The equilibrium potentials for the Al matrix, Mg_2Si , $AlFeSi$ and Si particles are -1080 , -1230 , -720 and -500 mV (versus SHE), respectively [39]. Thus, the $AlFeSi$ and Si particles are expected to be cathodic when compared to the Al matrix and Mg_2Si [39].

Mechanism of physical adsorption in case of 6063 aluminum alloy, may be explained as follows. In alkaline aqueous solution, a fraction of principal active constituents of TCE may exist in the deprotonated form [40] and remaining as neutral molecules. These deprotonated $-OH$ groups of the inhibitor molecules can get physically adsorbed on the positively charged sites and brings anodic reaction under control. The efficiency of inhibitor is more due to the large size of the active constituents, which exert umbrella effect. The inhibitor molecule is big enough to cover both anodic and cathodic area. As a result of this, both anodic and cathodic reactions come under control. Hence it acts as a mixed type of inhibitor, with more control over the anodic reaction.

3.6. SEM/EDX studies

Surface morphology studies help to understand the extent of adsorption of inhibitor molecule on the surface of the metal. The SEM images of corroded surface of 6063 aluminum alloy in 0.5 M NaOH is given in Fig. 7 (a). Fig. 7 (b) shows the SEM image of sample immersed in 0.5M NaOH containing of 500 ppm TCE. It is very much evident from Fig 7 (b) that surface has become soft and compact after the addition of inhibitor. This is due to the adsorption of inhibitor molecule on the metal surface.

Fig. 8 (a) represents EDX spectrum of the corroded sample of the 6063 aluminum alloy in 0.5 M NaOH. The spectrum shows peaks for aluminum, oxygen suggesting the presence of aluminum oxide/hydroxide and Peak for sodium represent the interaction of the metal with corrosive. Fig. 8 (b) depicts the EDX spectrum for the sample immersed in 0.5M NaOH containing of 500 ppm TCE Prominent peak for carbon indicates the adsorption of inhibitor molecule on the surface of the metal.

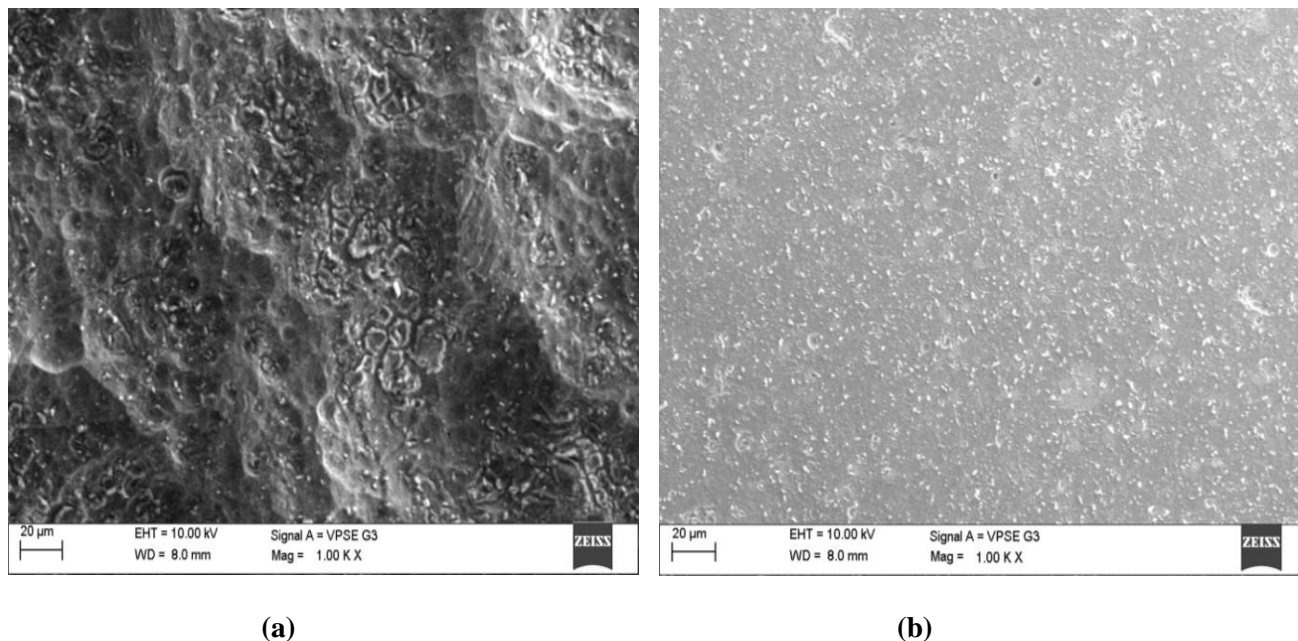


Figure 7: SEM image of (a) 6063 aluminium alloy in 0.5 M NaOH (b) 6063 aluminium alloy in 0.5 M NaOH + TCE (500 ppm)

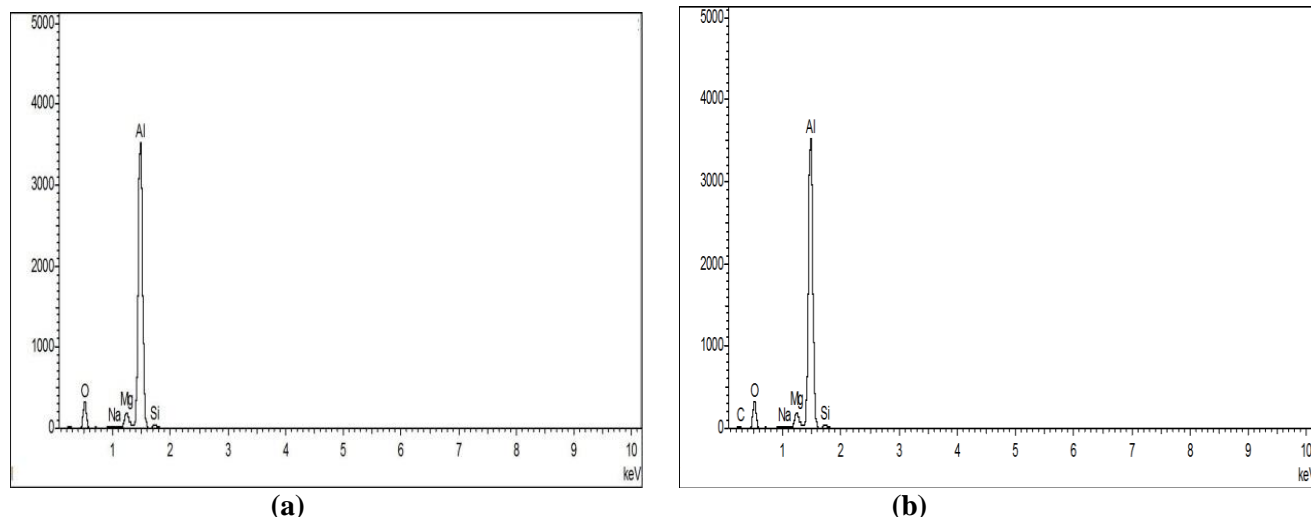


Figure 8: EDX spectrum of (a) 6063 aluminium alloy in 0.5 M NaOH (b) 6063 aluminium alloy in 0.5 M NaOH + TCE (500ppm)

Conclusions

- TCE acts as a good eco-friendly green inhibitor for the corrosion control of 6063 aluminum alloy in sodium hydroxide medium.
- Inhibition efficiency of the TCE increased with increase in the concentration of the inhibitor and decreased with increase in the temperature for both the materials.
- TCE acted as a mixed type of inhibitor and inhibitor obeyed Langmuir adsorption isotherm, the adsorption was through physisorption.
- Results obtained by weight loss method and potentiodynamic polarization method were in good agreement with one another.

Acknowledgements

- Mrs. Deepa Prabhu, acknowledges Manipal University, for the Fellowship, and Department of Chemistry MIT Manipal, for laboratory facilities.
- Both the authors gratefully acknowledge Prof. V. Aravinda Hebbar, Botanist Udipi, Karnataka, and Prof. A. N. Shetty, Professor, Department of Chemistry, NITK Surathkal, Karnataka for useful discussions.

ID 380217

References

1. Stansbury E.E, Buchanan R.A, Fundamentals of Electrochemical Corrosion, ASM International Materials Park, USA, 2000.
2. Vargel C, Corrosion of Aluminum, Elsevier, Oxford, 2004.
3. Deepa Prabhu, Padmalatha Rao, *Arabian Journal of Chemistry* (2014), <http://dx.doi.org/10.1016/j.arabjc.2013.07.059>.
4. Boukerche I, Djerad S, Benmansour L, Tifouti L, Saleh K., *Corrosion Science* 78 (2014) 343.
5. Reena Kumari P. D., Jagannath Nayak, Nityananda Shetty A., *J. Coat. Technol. Res.* 8 (6) (2011) 685.
6. Oguzie E.E, Okolue R, Oguke C.E, Unaegbu C, *Material Letters* 60 (2006) 3376.
7. Soliman H.N., *Corrosion Science* 53 (2011) 2994.
8. Reena Kumari P. D., Jagannath Nayak, Nityananda Shetty A., *J. Mater. Environ. Sci.* 2 (4) (2011) 387-402.
9. Deepa Prabhu, Padmalatha Rao, *J. Environ. Chem. Eng.* 1 (2013) 676.
10. Amitha Rani B.E., Bharathi Bai J.B., *Int. J. Corr.* (2012) ID 380217, <http://dx.doi.org/10.1155/2012/380217>.

11. Olusegun Abiola K., Otaigbe J.O.E., Kio O.J., *Gossipium hirsutum* L. extracts as green corrosion inhibitor for aluminum in NaOH solution, *Corrosion Science* 51 (2009) 1879.
12. Abdel-Gaber A.M., Khamis E., Abo-ElDahab H., Sh. Adeel, *Materials Chemistry and Physics* 109 (2008) 297.
13. Raja P.B., Sethuraman M.G., *Mater. Lett.* 62 (2008) 113.
14. Chia Lin Chang, Che San Lin, *Evidence-Based Complementary and Alternative Medicine* (2012), Article ID 125247. <http://dx.doi.org/10.1155/2012/125247>.
15. Handa S.S., Khanuja S.S., Longo G., Rakesh D., Extraction Technologies for Medicinal and Aromatic Plants, International Centre for Science and High Technology, Trieste, 2008.
16. Fontana M.D., Corrosion Engineering, McGraw-Hill, 3rdedn, Singapore, 1987.
17. Abiola O.K., Otaigbe J.O.E., *Corrosion Science* 50 (1) (2008) 242.
18. Li W., He Q., Zhang S., Pei C., Hou B., *J Appl Electrochem.* 38 (2008) 289.
19. Mohammad Javad Bahrami, Seyed Mohammad Ali Hosseini, *International Journal of Industrial Chemistry* 3 (2012) 30.
20. Mahendra Yadav, Usha Sharma, Premanand Yadav, *International Journal of Industrial Chemistry* 4 (2013) 6.
21. Abdel-Gaber A.M., Abd-El-Nabey B.A., Sidahmed I.M., El-Zayady A.M., Saadawy M., *Corrosion Science* 48 (2006) 2765.
22. Hegazy M.A., Ahmed H.M., El-Tabei A.S., *Corrosion Science* 53 (2011) 671.
23. Oguzie E.E., *Corrosion Science* 49 (2007) 1527.
24. Martinez S., Stern I., *Appl. Surf. Sci.* 199 (2002) 83.
25. Fekry A.M., Ameer M.A., *Int J Hydrogen Energy* 35 (2010) 7641.
26. Tao Z., Zhang S., Li W., Hou B., *Ind Eng Chem Res* 50 (2011) 6082.
27. Oguzie E.E., Njoku V.O., Enenebeak C.K., Akalezi C.O, Obi C, *Corrosion Science* 50 (2008) 3480.
28. Benali O., Benmehdi H., Hasnaoui O., Selles C., Salghi R., *J. Mater. Environ. Sci.* 4 (1) (2013) 127.
29. Selim I.Z., Khedr A.A., El-Shobki K.M., *J. Mater. Sci. Technol.* 12 (1996) 267.
30. Gao J., Weng Y., Salitanat, Feng L., Yue H., *Pet. Sci.* 6 (2009) 201.
31. Ekpe U.J., Ibok U.J., Ita B.I., Offiong O.E., Ebenso E.E., *Mater. Chem. Phys.* 40 (1995) 87.
32. Ambrish Singh, Singh V. K., Quraishi M. A., *J. Mater. Environ. Sci.* 1 (3) (2010) 162.
33. Ashok Kumar, Iniyavan P., Saravana Kumar M., Sreekanth A., *J. Mater. Environ. Sci.* 3 (3) (2012) 461.
34. Obot I.B., Umoren S. A, Obi-Egbedi N.O., *J. Mater. Environ. Sci.* 2 (1) (2011) 60.
35. Shivakumar S.S., Mohana K.N., *J. Mater. Environ. Sci.* 4 (3) (2013) 448.
36. Hammouti B., Zarrouk A., AL-Deyab S.S., Warad I., *Oriental Journal of Chemistry*, 27 (1) (2011) 23.
37. Benali O., Benmehdi H., Hasnaoui O., Selles C., Salghi R., *J. Mater. Environ. Sci.* 4 (1) (2013) 127.
38. Abiola O. K., Aliyu A.O.C., Phillips A.A., Ogunsipe A.O., *J. Mater. Environ. Sci.* 4 (3) (2013) 370.
39. Kaoru Mizuno, Anders Nylund, Ingemar Olefjord, *Corrosion Science* 43 (2001) 381.
40. Miadoková M., Petrtylová J., *Chem. Papers* 39 (2) (1985) 237.

(2015) ; <http://www.jmaterenvirosci.com>